

Assigning the transition from normal to local vibrational mode in SO_2 by periodic orbits

R. Prosmi^a, S.C. Farantos^{a,*}, H. Guo^b

^a Department of Chemistry, University of Crete, Iraklion, Crete 711 10, Greece

^b Department of Chemistry and Albuquerque High Performance Computer Center, University of New Mexico, Albuquerque, NM 87131, USA

Received 17 June 1999

Abstract

The bifurcation diagrams of periodic orbits are compared for three different potential functions of the ground electronic state of SO_2 . By assigning families of periodic orbits to overtone and combination vibrational levels of the symmetric stretch mode, the transition from normal- to local-type motions is identified to take place at the energy where the symmetric stretch family turns from stable to unstable and new local-type periodic orbits are generated. © 1999 Elsevier Science B.V. All rights reserved.

1. Introduction

The transition from a normal to a local vibrational mode in small polyatomic molecules has been observed and extensively discussed in the literature [1]. Lawton and Child [2] were among the first to carry out extensive studies on this subject. Particularly, they investigated the H_2O molecule with classical, semiclassical and quantum-mechanical theories using simple model potentials and this allowed the investigators to examine the role of the potential and kinetic coupling terms carefully.

In this work, Lawton and Child predicted normal-mode behaviour for SO_2 , since a normal-mode model was found to describe successfully the

low-lying vibrational states. However, spectroscopic studies and calculations by Yamanouchi and coworkers [3–5] showed that, in the ground electronic state, the vibrational levels $(n_1, 0, 0)$ and $(n_1 - 1, 0, 1)$ form the characteristic doublets expected in local-mode vibrational behaviour. The three numbers in the parentheses denote the number of quanta in the symmetric stretch, bend and antisymmetric stretch in a normal-mode-type assignment, respectively. By fitting the energies of 311 vibrational levels obtained from dispersed fluorescence spectra to an algebraic Hamiltonian, they extracted wavefunctions the morphologies of which offer an undisputable assignment [5] of the normal and local states. The dispersed fluorescence spectra were obtained from transitions between the excited ($\tilde{\text{C}}^1\text{B}_2$) and ground electronic state ($\tilde{\text{X}}^1\text{A}_1$).

A periodic orbit (PO) investigation of the vibrational motions of SO_2 as well as a classical mechanical simulation of the ($\tilde{\text{C}}^1\text{B}_2 \rightarrow \tilde{\text{X}}^1\text{A}_1$) spectroscopic

* Also at Institute of Electronic Structure and Laser, FORTH, Iraklion, Crete 711 10, Greece. Corresponding author. Fax: +30-81-39-1305; e-mail: farantos@iesl.forth.gr

transitions were carried out in our laboratory [6,7] some time ago using an empirical [8] and an ab initio [9] potential energy surface. It was found that the empirical potential shows a transition to irregular motions around 1.7 eV above the minimum of the potential, mainly due to the coupling of the symmetric stretch and bend vibrational modes. The Murrell–Sorbie potential function used was too soft in the bend coordinate compared to the ab initio surface.

Recently, extended quantum-mechanical calculations were carried out by Guo and coworkers [10–12] using the spectroscopic potential of Kauppi and Halonen [13]. This potential is expressed in terms of the bend angle and Morse radial variables and reproduces the experimentally observed energy levels up to high energies. The characteristic of the new vibrational studies on SO_2 is the size of the calculations, since the researchers were able to compute about 4700 vibrational eigenenergies spanning an energy range up to $25\,000\text{ cm}^{-1}$. They efficiently applied filter diagonalization algorithms [14–16] to compute the eigenenergies in certain energy windows. Statistical analysis of the energy level spacing distributions showed largely regular behaviour [17].

The theme on the transition from a normal to a local mode of the symmetric stretch of SO_2 molecule was addressed in a separate publication by the same authors [11]. What came up in this study was the difficulty in defining the transition energy and it was

suggested that the transition from a normal to a local mode is completed at about $25\,000\text{ cm}^{-1}$ above the zero-point energy. This conclusion was based on the almost double degeneracy of the $(n_1, 0, 0)$ and $(n_1 - 1, 0, 1)$ levels which is reached at about this energy.

In several previous studies, we have argued that families of POs [18,19], and especially continuation/bifurcation (C/B) diagrams of them, are suitable for the assignment of vibrational overtone states and that they can reveal resonances which are sometimes difficult to characterize [20,21]. The aim of this Letter is to show that, by constructing the C/B diagrams of the POs [18,22] of SO_2 , and assigning the proper families to the overtone and combination levels, we can predict and define the transition energy from the normal to the local mode as the bifurcation energy of the symmetric stretch family. Periodic orbits have been located for three different potential functions of the ground electronic state of SO_2 and, thus, it is interesting to compare the bifurcation diagrams extracted from them to see how the dynamics change by modifying the potential energy surfaces.

2. Results and discussion

C/B diagrams of POs have been constructed for three different potential functions of the ground elec-

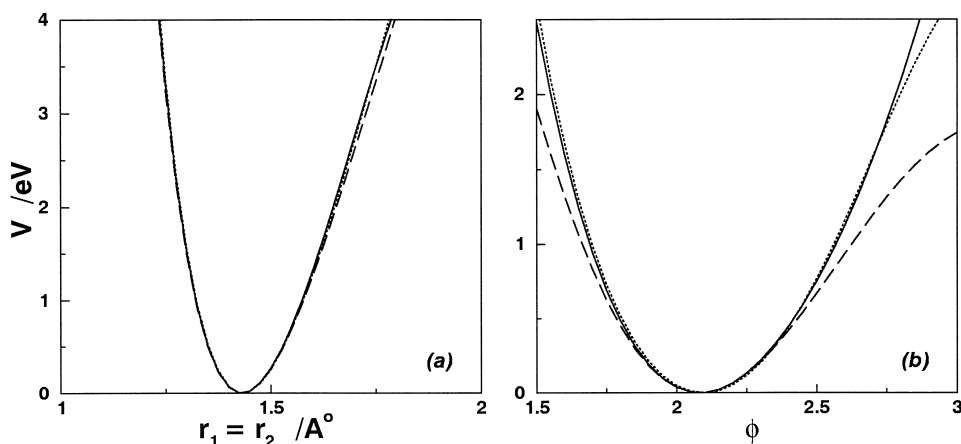


Fig. 1. Comparison of the spectroscopic potential of Kauppi and Halonen [13] (solid lines) with the ab initio surface of Weis [9] (dotted lines) and with the empirical Murrell–Sorbie function [8] (dashed lines).

tronic state: a global potential based on the Murrell–Sorbie many-body approach [8], which is a function of the three interatomic bond lengths and it interpolates bound and unbound states of the molecule. The second potential examined was a polynomial expansion in properly scaled coordinates of the SO bond lengths and the angle between them and fitted to *ab initio* calculations [9]. The *ab initio* points covered a grid of (1.2, 1.8) Å for the SO bond

lengths, r_1 and r_2 , and the range of (70°, 130°) for the angle ϕ between them. Finally, the third potential is a spectroscopic potential [13] expressed in terms of the bond angle ϕ and Morse-type functions for the stretches. The parameters in this potential were fitted to experimental vibrational levels. In Fig. 1, we compare the three potentials by plotting the energy as a function of the SO bond lengths in C_{2v} geometries (Fig. 1a) and as a function of the angle ϕ

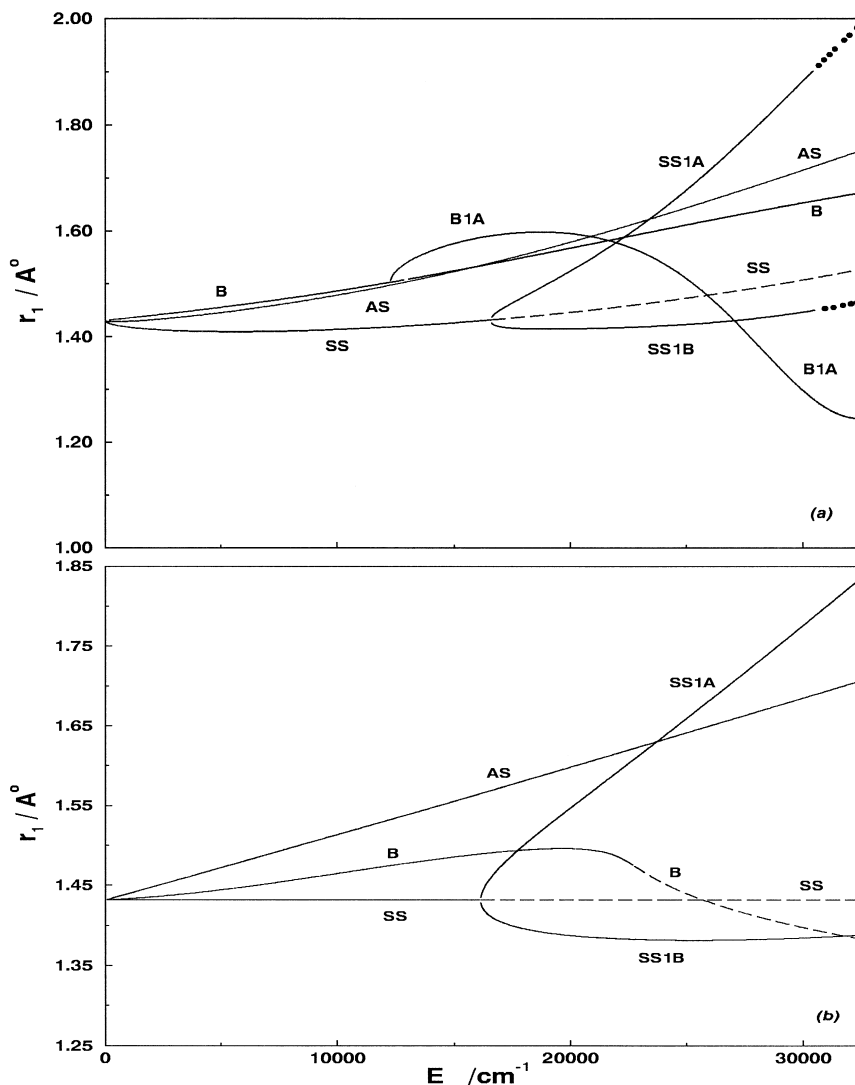


Fig. 2. C/B diagrams for the principal families emanating from the minimum of (a) Kauppi and Halonen potential and (b) *ab initio* surface of Weis. SS is the symmetric stretch family, AS the asymmetric stretch and B the bend family of POs. Solid lines denote stable POs, dashed lines unstable and the dotted lines complex unstable POs.

keeping the bond lengths $r_1 = r_2 = 1.4308 \text{ \AA}$ (Fig. 1b). We can see from this figure that there is a good agreement among the three potentials in the stretch modes up to energies of 3 eV (Fig. 1a), but there are substantial deviations among them in the bend coordinate starting at the energy of 0.5 eV (Fig. 1b). The spectroscopic potential of Kauppi and Halonen is denoted by solid lines: the ab initio one with dotted lines and the Murrell–Sorbie potential by dashed lines. It turns out that, in the bend coordinate, there is better agreement between the spectroscopic and ab initio potential surfaces than the Murrell–Sorbie function which is much softer for both small and large angles.

The projection of the C/B diagram in (E, r_1) plane for the Murrell–Sorbie potential function has been presented in our previous publication (see Fig. 7 in Ref. [7]). We remind that in such plots we show the initial conditions of the located POs at different total energies E which act as the control parameter in the continuation process. In Fig. 2a,b we show similar graphs for the Kauppi and Halonen and ab initio potentials, respectively.

B denotes the family of POs which is associated with the bend mode, **SS** is the family associated with the symmetric stretch mode and **AS** the asymmetric stretch family. As can be seen in Fig. 2 POs have been located up to 32000 cm^{-1} . For both surfaces the **AS** family remains stable (solid lines) for the total energy interval. The **B** family for the spectroscopic function bifurcates at the energy of 12280 cm^{-1} giving birth to POs with a double period, and it remains unstable up to 13035.5 cm^{-1} , it then turns to stable for the rest of the energy range up to 32000 cm^{-1} . For the ab initio potential, the **B** family turns to single unstable at 20265.6 cm^{-1} , it becomes stable at 20749.5 cm^{-1} , and finally, it turns to single unstable at 22765.9 cm^{-1} (dashed line).

The **SS** family turns from stable to single unstable (dashed lines) at the energies of 16639 and 16150 cm^{-1} for the spectroscopic and ab initio surfaces, respectively. This gives birth to a bifurcation of two new families of POs with the same period as the parent one. This bifurcation signals the transition to local type motions (see Fig. 5). The bifurcating **SS1A/B** families turn to complex unstable POs (dotted lines) at about 30550 cm^{-1} for the spectroscopic potential.

In Fig. 3 plots of the periods of the principal families of POs as functions of the total energy are presented for the three potentials. The results from the spectroscopic potential are denoted by solid lines, those from the ab initio potential with dotted lines and the periods of the Murrell–Sorbie potential by dashed lines. We note that the bifurcation to local-type POs was marked with the label **SS2** in our previous publication and we keep the same symbol here.

The Murrell–Sorbie and the spectroscopic potential show very similar behaviour in the stretch modes. The asymmetric stretch family is stable and the bifurcations of the symmetric stretch families are

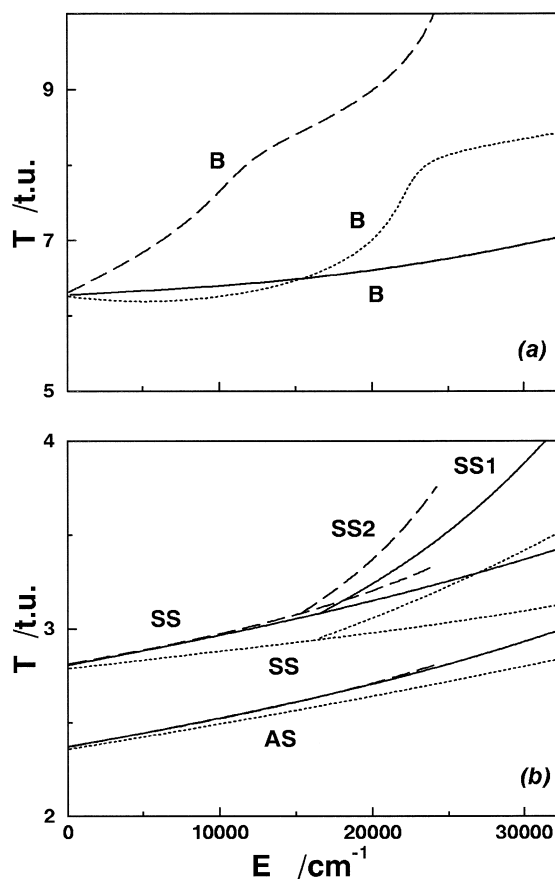


Fig. 3. The periods of the principal families of POs as a function of the total energy for the spectroscopic (solid lines), ab initio (dotted lines) and empirical (dashed lines) potential surfaces. T is the period of POs in time units ($1 \text{ t.u.} = 1.018 \times 10^{-14} \text{ s}$). The notation for the POs is the same as in Fig. 2 and Fig. 7 in Ref. [7].

also reproduced. In spite of the good agreement among the three potentials in the stretch modes shown in Fig. 1a, there are substantial deviations in the periods extracted from the ab initio potential. Such trends can be understood since the spectroscopic and the Murrell–Sorbie potentials were fitted to experimental spectra whereas the ab initio potential reflects the quality of the quantum chemistry calculations which apparently have not reached spectroscopic accuracy.

Differences are mainly found in the bending mode (Fig. 3a). The Murrell–Sorbie potential function does not reproduce very well the potential in the bend coordinate and this results in an early transition to irregular behaviour, around 1.7 eV above the minimum. For the ab initio surface, the irregularity appears at energies above 2.5 eV and for the spectroscopic one there is only a short energy range of 0.1 eV around 1.5 eV above the minimum where the bend mode is unstable. The behaviour of the Murrell–Sorbie potential is expected, since it is the only one which gives a global description of the nuclear

configuration space of the molecule. The poor agreement of highly excited bend levels with experimental ones strengthens the case that the linearity and the isomerization channel influence the vibrational levels at these energies.

Weston and Child [23] have studied the normal-to-local transition in symmetric triatomic molecules, AB_2 , using a model of kinetically coupled Morse oscillators. The investigators were able, by reducing the problem to Hill's equation, to extract a scaling relation for the transition from stable to unstable motions based on the stretch frequencies ratio and the reduced energy (E/D), scaled with respect to the dissociation energy, D . Applying their formula to the SO_2 molecule, we predict that for a ratio of fundamental stretch frequencies (ω_3/ω_1) of roughly 1.18, the onset of the bifurcation is estimated at about 0.4 times of the dissociation energy which is $45\,573\text{ cm}^{-1}$. This estimate of $18\,229\text{ cm}^{-1}$ is an upper bound to our results shown in Fig. 2, which identifies the bifurcation energy at $16\,639$ and $16\,150\text{ cm}^{-1}$ for the spectroscopic and ab initio surfaces,

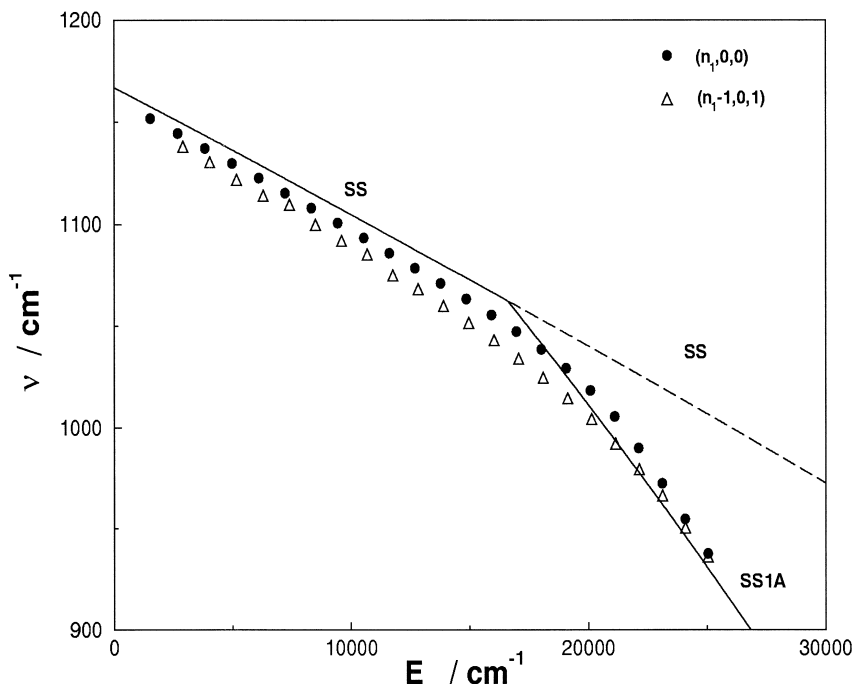


Fig. 4. Energy differences between successive energy levels of the $(n_1, 0, 0)$ overtones (filled circles) and $(n_1 - 1, 0, 1)$ (triangles) combinations. The lines represent the frequencies obtained from the POs of the SS family and its bifurcation SS1. To compare classical and quantum results, we shift the quantum mechanical vibrational levels by the zero-point energy.

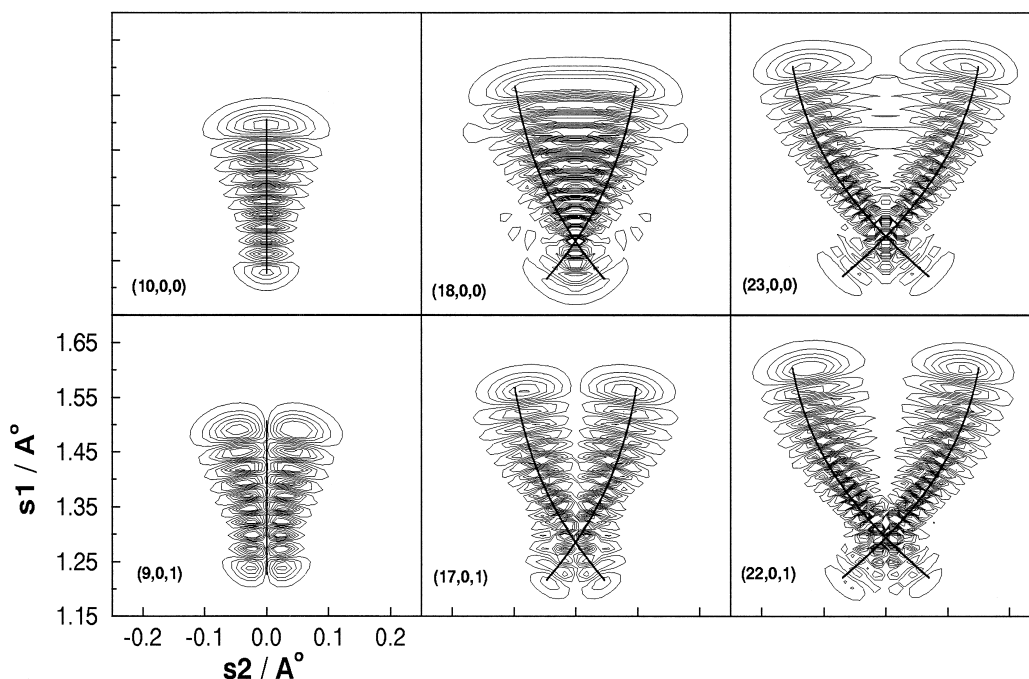


Fig. 5. Contour plots of vibrational eigenfunctions of SO_2 and projections of POs of the **SS** and **SS1** families in configuration space. The coordinates s_1, s_2 are the symmetrized and antisymmetrized Radau coordinates, respectively.

respectively. In Fig. 4, we plot the energy differences of successive energy levels, computed by Guo and coworkers [10–12], of the type $(n_1, 0, 0)$ (filled circles) and $(n_1 - 1, 0, 1)$ (triangles) as functions of the total energy for the spectroscopic surface. The lines represent the classical frequencies (ν) in wavenumbers obtained from the periods (T) of the **SS** and **SS1A** families. For the comparison of classical and quantum mechanical results, we have shifted the quantum vibrational levels by the zero-point energy.

Finally, in Fig. 5 representative wavefunctions with the POs superimposed are shown to demonstrate the correspondence of local-type wavefunctions with the **SS1A/B** POs. The coordinates used in the quantum-mechanical calculations are the symmetric (s_1) and the antisymmetric (s_2) combinations of the Radau stretch coordinates.

From Fig. 4, we see that the classical frequency curves smoothly interpolate the quantum-mechanical points. At low and high total energies, the energy differences of the $(n_1, 0, 0)$ and $(n_1 - 1, 0, 1)$ levels are small with the maximum gaps among them occurring

close to the bifurcation point. Although quantum-mechanically there is no sharp transition from the normal- to the local-type mode, the correspondence of the eigenfunctions to the POs legitimizes our defining as the critical transition energy the bifurcation energy of the **SS** family.

3. Conclusions

Summarizing our results, we can state that in spite of the differences among the three potential energy surfaces used to describe the electronic ground state of SO_2 , the general trends in the C/B diagrams are reproduced. However, there are quantitative differences when we examine the bifurcation energies especially in the bend mode, a coordinate related to isomerization paths of the molecule. It turns out that the Murrell–Sorbie potential is less accurate in the bend coordinate, whereas the ab initio surface lacks in reproducing the overtone frequencies.

By assigning the bifurcating family of POs, **SS1A/B**, to the combination levels $(n_1 - 1, 0, 1)$, we pro-

pose that as the transition energy from the normal- to the local-type motion can be adopted the bifurcation energy of **SS** and the genesis of **SS1A/B**. This energy is $16\,639\text{ cm}^{-1}$ for the spectroscopic and $16\,150\text{ cm}^{-1}$ for the ab initio potential. The analytical formula of Weston and Child estimates this energy at $18\,229\text{ cm}^{-1}$.

A similar PO bifurcation analysis was carried out for O_3 [24] and acetylene [25] molecules, which also show a transition from normal to local stretch motions. It turns out that the PO assignment not only elucidates this type of phenomena, but it can also generalize the concept of the normal-to-local mode transition. For example, a bifurcation analysis of POs of T-shaped Ar_3 at the saddle point for the inversion of the axial argon atom has shown that a transition from normal (unstable motion) to local (stable motion) is taking place [26].

Acknowledgements

R.P. gratefully acknowledges a TMR Fellowship, under Contract ERBFMBICT98 3429; H.G. is supported by NSF (CHE-9713995). We thank Prof. Child for bringing Ref. [23] to our attention.

References

- [1] L. Halonen, in: *Advances in Chemical Physics*, vol. 104, Wiley, New York, 1998, pp. 41–179.
- [2] R.T. Lawton, M.S. Child, *Mol. Phys.* 44 (1981) 709.
- [3] K. Yamanouchi, H. Yamada, S. Tsuchiya, *J. Chem. Phys.* 88 (1988) 4664.
- [4] K. Yamanouchi, S. Takeuchi, S. Tsuchiya, *J. Chem. Phys.* 92 (1990) 4044.
- [5] T. Sako, K. Yamanouchi, *Chem. Phys. Lett.* 264 (1996) 403.
- [6] S.C. Farantos, *Laser Chem.* 13 (1993) 87.
- [7] R. Prosmiiti, S.C. Farantos, H.S. Taylor, *Mol. Phys.* 82 (1994) 1213.
- [8] J.N. Murrell, S. Carter, S.C. Farantos, P. Huxley, A.J.C. Varandas, *Molecular Potential Energy Functions*, Wiley, New York, 1984.
- [9] B. Weis, Ph.D. Thesis, University of Frankfurt, Main, 1992.
- [10] G. Ma, R. Chen, H. Guo, *J. Chem. Phys.* 110 (1999) 8408.
- [11] G. Ma, H. Guo, *J. Chem. Phys.* (1999) in press.
- [12] D. Xie, G. Ma, H. Guo, *J. Chem. Phys.* (1999) in press.
- [13] E. Kauppi, L. Halonen, *J. Chem. Phys.* 96 (1992) 2933.
- [14] V.A. Mandelshtam, H.S. Taylor, *J. Chem. Phys.* 106 (1997) 5085.
- [15] V.A. Mandelshtam, H.S. Taylor, *J. Chem. Phys.* 107 (1997) 6756.
- [16] R. Chen, H. Guo, *Chem. Phys. Lett.* 279 (1997) 252.
- [17] M.C. Gutzwiller, *Chaos in Classical and Quantum Mechanics*, vol. 1, Springer, Berlin, 1990.
- [18] S.C. Farantos, *Int. Rev. Phys. Chem.* 15 (1996) 345.
- [19] J.M. Gomez Llorente, E. Pollak, *Annu. Rev. Phys. Chem.* 43 (1992) 91.
- [20] S.C. Farantos, H.-M. Keller, R. Schinke, K. Yamashita, K. Morokuma, *J. Chem. Phys.* 104 (1996) 10055.
- [21] Ch. Beck, H.-M. Keller, S.Yu. Grebenshchikov, R. Schinke, S.C. Farantos, K. Yamashita, K. Morokuma, *J. Chem. Phys.* 107 (1997) 9818.
- [22] S.C. Farantos, *Comp. Phys. Comm.* 108 (1998) 240.
- [23] T. Weston, M.S. Child, *Chem. Phys. Lett.* 262 (1996) 751.
- [24] M.E. Kellman, *J. Chem. Phys.* 83 (1985) 3843.
- [25] R. Prosmiiti, S.C. Farantos, *J. Chem. Phys.* 103 (1995) 3299.
- [26] R. Guantes, A. Nezis, S.C. Farantos, *J. Chem. Phys.* (1999) submitted.